Simulation of rainbows, coronas, and glories by use of Mie theory

Philip Laven

Mie theory offers an exact solution to the problem of scattering of sunlight by spherical drops of water. Until recently, most applications of Mie theory to scattering of light were restricted to a single wavelength. Mie theory can now be used on modern personal computers to produce full-color simulations of atmospheric optical effects, such as rainbows, coronas, and glories. Comparison of such simulations with observations of natural glories and cloudbows is encouraging. © 2003 Optical Society of America

OCIS codes: 010.1290, 290.4020.

1. Introduction

Scattering of sunlight by spherical drops of water may seem to be a relatively simple process, but it causes a surprising variety of complicated optical effects, such as primary and secondary rainbows, coronas, and glories—some of which, even today, are not fully understood. In the seventeenth century Descartes and Newton used geometrical optics to explain the formation of rainbows.[1,2] In 1838 Airy[3] extended the earlier theories by including the effects of diffraction and interference, thus explaining the formation of the rainbow's supernumerary arcs that are not predicted by geometrical optics.

In 1908 Gustav Mie[4] provided a rigorous solution to the problem of scattering of electromagnetic plane waves by a homogeneous sphere. However, for many years this theory seemed to have little practical value because it was computationally demanding. H. C. van de Hulst published a bibliography[5] of Mie results available in 1957. Such results were mainly in the form of tables of computed values for small drops with size parameter $x < 30$ ($x = 2\pi r/\lambda$ where r is the drop radius and λ is the wavelength of the incident light). H. C. van de Hulst also published[6] some graphs of intensity versus scattering angle for $1 \leq x \leq 5$. For scattering of light from water drops in the atmosphere we are interested in much larger values of x, perhaps from $x = 50$ for fog droplets to $x > 10{,}000$ for rain during thunderstorms. Because Mie theory becomes even more forbidding for large spheres, significant effort has been spent on searching for approximations to Mie theory.[7–9] Eventually, the increasing power of computers and the development of efficient computer algorithms[10,11] permitted wider use of Mie theory,[12–16] but such use was generally restricted to scattering of light of a single wavelength. However, it was not until the late 1990s that Mie theory was, at last, used to simulate atmospheric optical effects in color.[17–19]

The research described here was initiated as a direct result of Lee's seminal paper[17] in which he compared simulations of rainbows using Mie theory and Airy theory. With the potential of modern personal computers with good-quality color displays, a computer program for Mie scattering of light has been developed. Based on the algorithm of Bohren and Huffman,[11] the MiePlot program can provide full-color simulations of optical effects caused by spherical water drops, such as rainbows, coronas, and glories. It can also produce a wide range of graphs of scattered intensity for perpendicular and/or parallel polarizations as functions of r, λ, scattering angle θ, and refractive index n. This program, which runs under Microsoft Windows, can be downloaded at no charge from http://www.philiplaven.com/mieplot.htm.

An example of the graphical output of the MiePlot program is given in Fig. 1, which demonstrates that Mie scattering of monochromatic light is very dependent on the size of the water drops. For light of wavelength 0.65 μm, scattering from a spherical drop with $r = 1000$ μm or $r = 100$ μm produces a primary rainbow at approximately $\theta = 138°$ and a secondary

P. Laven (philip@philip.laven.com) can be reached c/o the European Broadcasting Union, Ancienne Route 17A, CH-1218 Grand Saconnex, Geneva, Switzerland.

Received 16 January 2002; revised manuscript received 25 March 2002.

0003-6935/03/030436-09$15.00/0

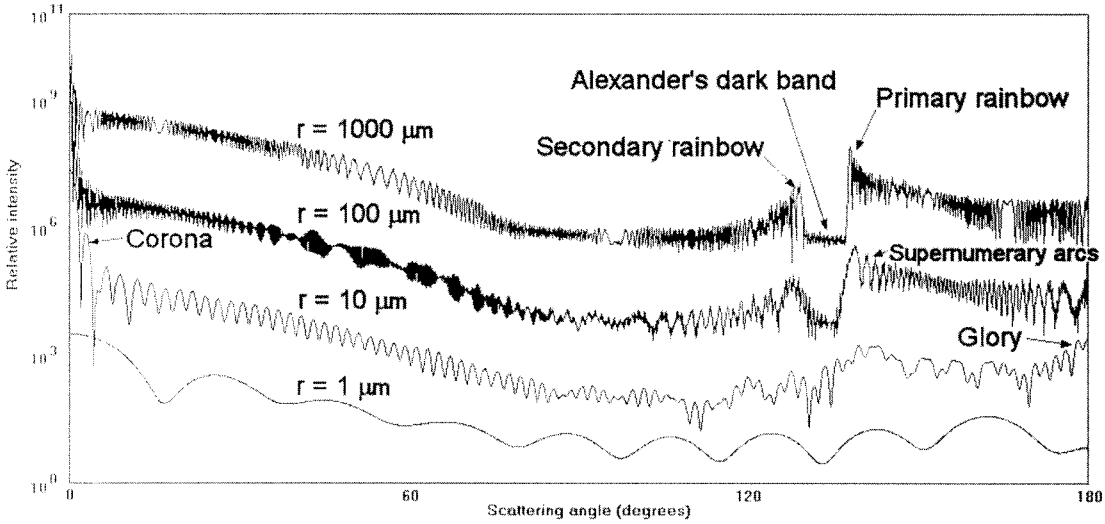

Fig. 1. Graphs of intensity versus scattering angle θ. Radius of spheres $r = 1$, 10, 100, and 1000 μm; wavelength of light $\lambda = 0.65$ μm; refractive index $n = 1.332$; unpolarized light.

rainbow at approximately $\theta = 129°$, together with Alexander's dark band between them. Other features, such as the corona for $\theta < 10°$ and the glory for $\theta > 170°$, are visible on the curve for $r = 10$ μm. The calculations of intensity as a function of θ were made at intervals of 0.1° for Fig. 1, but all other calculations reported in this paper used an interval of 0.01°.

2. Simulation of Rainbows

Figure 2(a) shows Mie scattering of monochromatic light from a drop with $r = 100$ μm for θ between 137° and 145°. Anyone familiar with Airy theory will probably consider the high-frequency ripples to be unnatural, but such ripples might be observable under laboratory conditions of monochromatic light scattered from a single drop. These ripples are mainly the result of interference between rays that have undergone one internal reflection ($p = 2$) and rays that have undergone one external reflection ($p = 0$).[20,21] Airy theory does not predict such ripples on the primary rainbow, because it ignores anything other than $p = 2$ rays.

Atmospheric optical effects are caused not by a single water drop but by millions of water drops of nonuniform size. Figure 2(b) shows the result of averaging the Mie intensities from 50 drops with a log-normal size distribution with a median radius of 100 μm and a standard deviation of 0.1 μm (0.1% of the median radius). Although this size variation is extremely small, it has a dramatic effect: Comparison of Figs. 2(a) and 2(b) shows that scattering from drops of nonuniform size removes the high-frequency ripples.

Natural atmospheric optical effects are caused by the Sun or the Moon, which are circular light sources with an apparent diameter of ~0.5°. Because Mie theory assumes a plane wave, it is necessary to integrate the intensities resulting from the Mie calculations over the diameter of the light source. Applying this additional step to the curve shown in Fig. 2(a) produces the monodisperse intensity curve shown in Fig. 2(c), where the high-frequency ripples have almost been removed.

Figure 2 is based on illumination by monochromatic light, whereas light from the Sun has a continuous broad spectrum. To simulate the spectrum of sunlight, the MiePlot program performs calculations at N equally spaced wavelengths between 0.38 and 0.7 μm (where the value of N can be selected by the user). The relative intensity of each wavelength is based on the measured solar spectral radiance shown in Fig. 3 of Lee's paper.[17] Although it can be argued that this spectral illuminant is not ideal because the Sun's elevation was 45°, it was adopted because it facilitated comparisons with Lee's results.

Figures 3(a) and 3(b) show the relative luminance curves resulting from addition of Mie calculations for $N = 10$ and $N = 1000$, respectively. These curves are similar in shape, but the curve for $N = 10$ has a complicated ripple structure, which is caused by the fact that the high-frequency ripples for monochromatic light vary rapidly with changing wavelength. When intensity curves for different wavelengths are added together, the ripple structure will be reinforced if the maxima and minima for the various wavelengths coincide; for example, the ripples shown in Fig. 2(a) for $\lambda = 650$ nm coincide approximately with those for $\lambda = 650.9$ nm, 651.8 nm, and so on. Figure 3(b) indicates that the ripple structure almost disappears for $N = 1000$, but this value of N is very large by normal colorimetric standards.

Figure 4 shows intensity curves plotted on a logarithmic scale for primary and secondary rainbows for $r = 100$ μm. This figure shows that the intensity for perpendicular polarization is generally much greater than for parallel polarization. An important exception occurs near the minima of the primary rainbow's

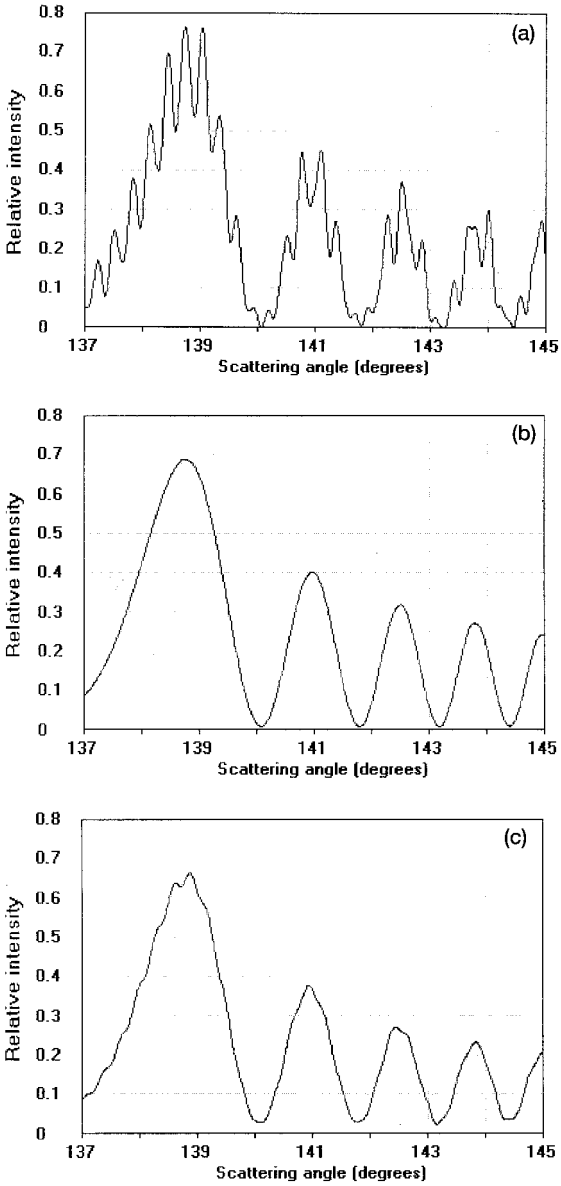

Fig. 2. (a) Graph of intensity versus scattering angle θ. $r = 100$ μm, $\lambda = 0.65$ μm, $n = 1.332$, perpendicular polarization. (b) As in (a) but intensity is the average intensity of scattering by 50 spheres with different values of radius with a log-normal distribution with a median radius of 100 μm and a standard deviation of 0.1 μm (0.1% of the median radius). (c) As in (a) but intensity is averaged to take account of the 0.5° diameter of the Sun.

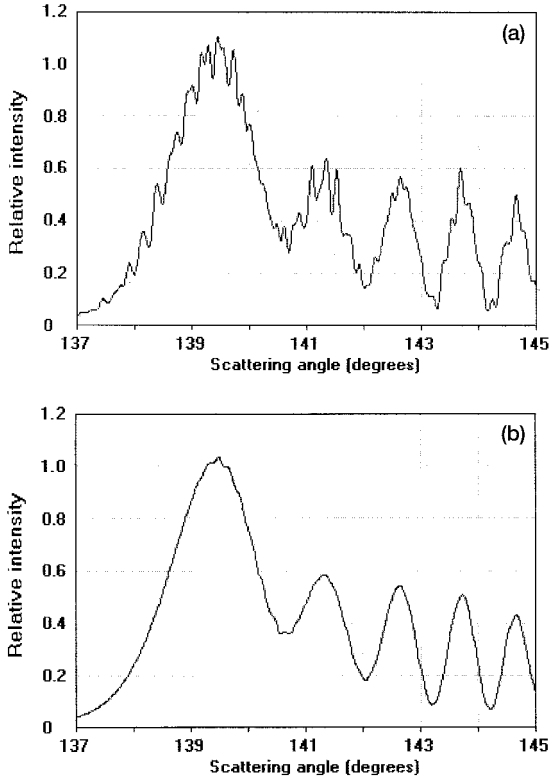

Fig. 3. (a) Graph of intensity versus scattering angle θ. $r = 100$ μm, ten values of λ equally spaced between 0.38 and 0.7 μm, n varies as function of λ, perpendicular polarization. (b) As in (a) but with 1000 values of λ equally spaced between 0.38 and 0.7 μm.

supernumeraries, which coincide with maxima of the supernumeraries for parallel polarization.[22]

Figure 4 was calculated with $N = 2000$ to avoid any problems with the ripple structure. For each value of θ, the intensity curve is the sum of the intensities for each of the 2000 wavelengths. Color simulations require the scattered intensities for each wavelength to be converted into RGB (red, green, blue) values used by computer displays. For each value of θ, the gamma-corrected sum of the resulting RGB values is used to generate the three horizontal stripes above the graph in Fig. 4, which represent the brightness and the color of light at specific values of θ: The top stripe is for perpendicular polarization, the middle stripe for parallel polarization, and the bottom stripe for unpolarized light. Since rainbows are strongly polarized, most of the middle stripe is very dark.

Figure 5 shows the results of an exercise to determine the minimum value of N for Mie simulations of the primary and secondary rainbows for $r = 100$ μm. Each horizontal stripe shows the results of calculations by use of a specific value of N. Figure 5(a) demonstrates that simulations of the primary rainbow (i.e., between $137° < \theta < 145°$) are fairly consistent for $10 < N < 2000$. Nevertheless, because there are some subtle variations when $N < 30$, it is suggested that $N = 30$ would be a safe choice for the primary rainbow when $r = 100$ μm. The secondary rainbow is shown in greater detail in Fig. 5(b), which indicates the need for even higher values of N (e.g., 600) to avoid visible ripples on such simulations. This discrepancy in the required value of N is due to differences in the ripple structures: Successive maxima of the ripples are separated by ~0.15° on the primary rainbow, compared with ~0.6° on the secondary rainbow. The smoothing effect caused by the 0.5° diameter of the Sun effectively removes the 0.15° ripples but has no effect on the 0.6° ripples. Consequently, more wavelengths are needed to suppress the visibility of the ripple structure on simulations of the secondary rainbow.

Lee[17] introduced a powerful technique to illustrate

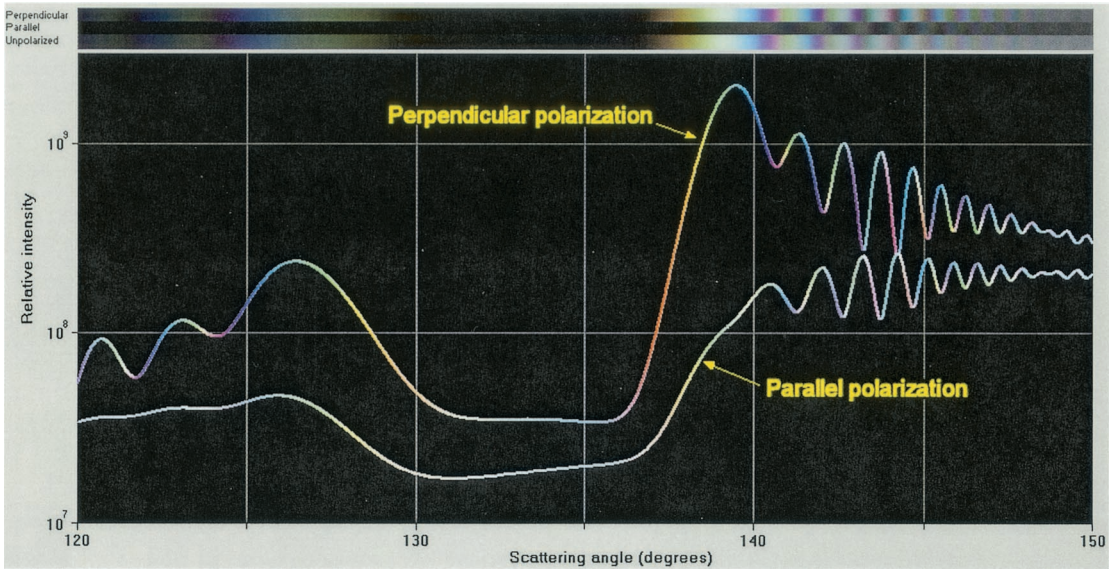

Fig. 4. Graph of intensity versus scattering angle θ for $r = 100$ μm, together with colored stripes simulating primary and secondary rainbows for perpendicular polarization, parallel polarization, and for unpolarized light ($N = 2000$).

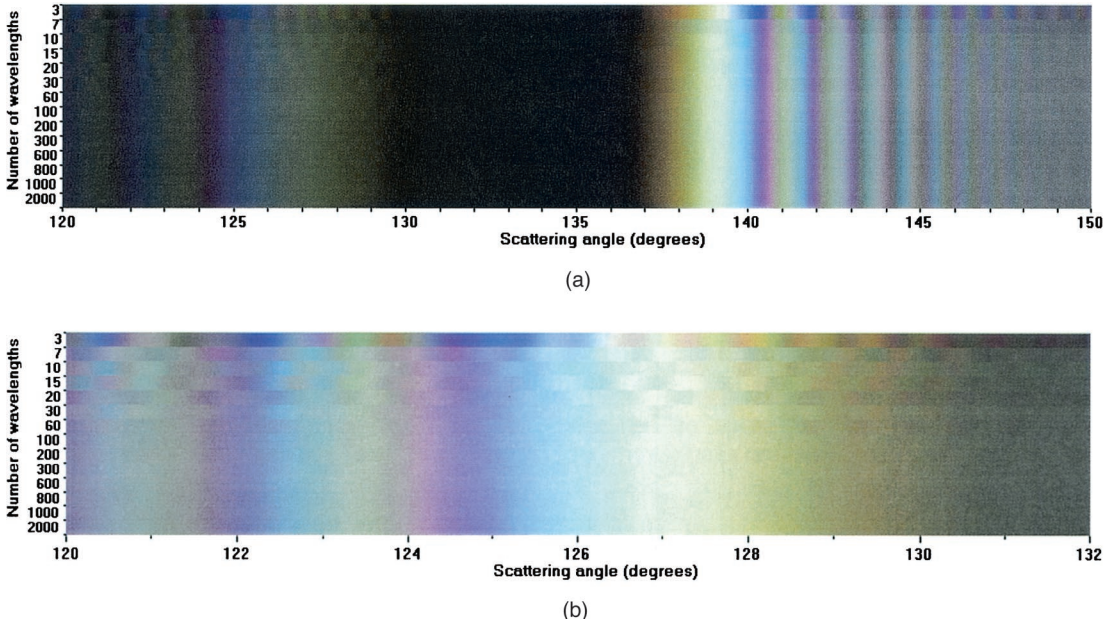

Fig. 5. (a) Simulation of primary and secondary rainbows caused by scattering of unpolarized sunlight from $r = 100$ μm water drops with the specified number N of wavelengths. (b) As in (a) but limited to the secondary rainbow.

how the appearance of rainbows varies with drop size. The MiePlot program can also generate these Lee diagrams, as shown in Fig. 6 where each colored point represents the color of light scattered in a specific direction θ by a drop of radius r. The brightness of each vertical line of colors representing the rainbow caused by a drop of radius r has been normalized by the maximum luminance for that value of r. Figure 6 is based on the assumption that the Sun is the light source, which implies that the Mie calculations have been smoothed to take account of the 0.5° apparent diameter of the Sun.

Figure 6 can be compared with Fig. 15 of Lee's paper[17]: As Lee noted, the latter's "only literally unnatural feature seems to be the Mie map's ripple structure, which appears as a subtle color marbling on the cloudbow primaries and their supernumeraries" (Ref. 17, p. 1514). Severe marbling is visible in Fig. 6, which was calculated with $N = 7$ for all values of r between 10 and 1000 μm, but Fig. 7 does not exhibit such marbling. The value of N used in production of Fig. 7 was a function of drop size: $N = 600$ for $r = 10$ μm drops, reducing to $N = 30$ for $r = 200$ μm drops or larger. Comparison of Figs. 6 and 7 demonstrates that marbling on such simulations can be avoided by use of higher values of N. It seems

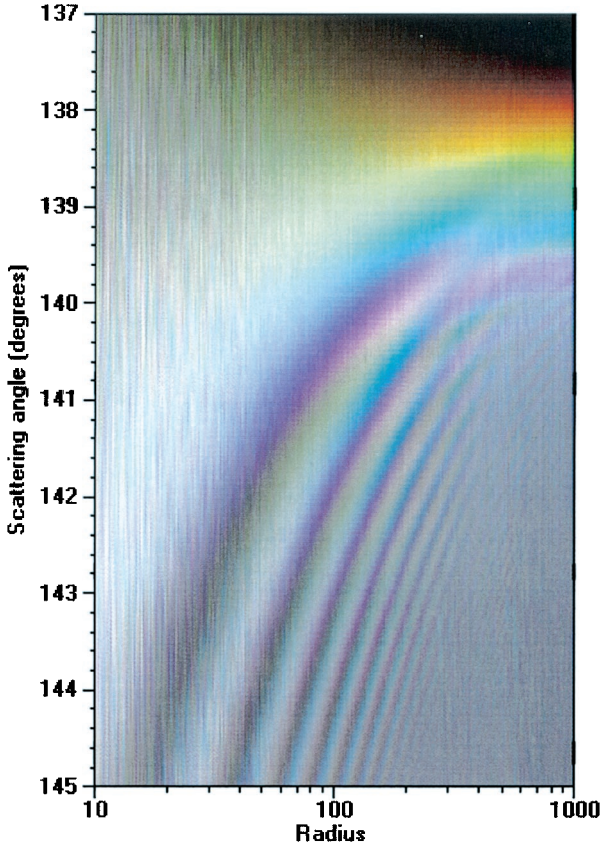

Fig. 6. Lee diagram of the primary rainbow for values of r between 10 and 1000 μm for unpolarized sunlight ($N = 7$).

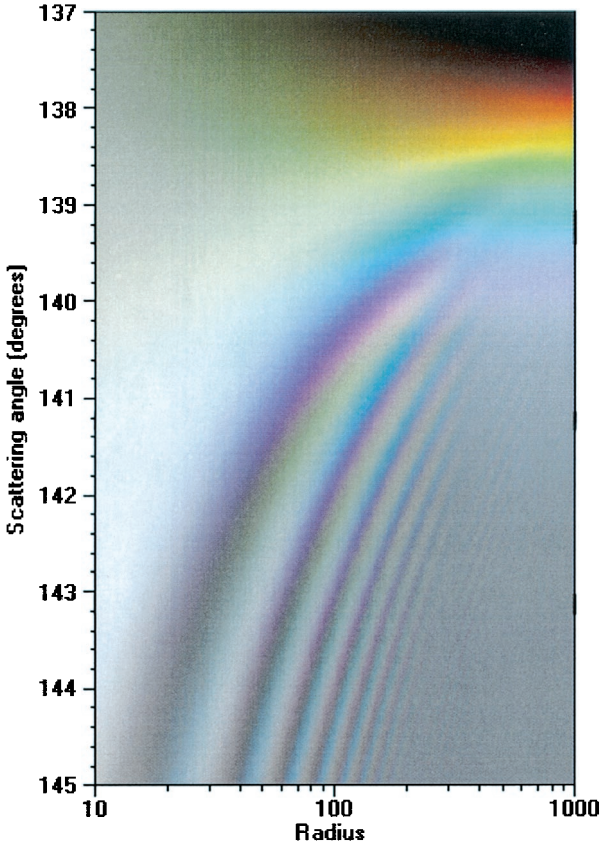

Fig. 7. Lee diagram of the primary rainbow for values of r between 10 and 1000 μm for unpolarized sunlight ($N = 6000/r$ for 10 μm $< r <$ 200 μm and $N = 30$ for $r >$ 200 μm).

that marbling is another manifestation of the ripples discussed above. Because the ripples occur at different values of θ for different values of r, they appear on Lee diagrams as lighter (or darker) diagonal stripes.

From the foregoing it is obvious that Mie theory can be demanding in terms of the number of wavelengths required when it is used to simulate the scattering of a continuous spectrum. It is important to understand that this is not due to the spectral characteristics of the incident light, such as sunlight. Similar problems occur even with a flat spectrum. The fundamental cause is that the high-frequency ripples correctly predicted by Mie theory for monochromatic light disappear when monochromatic light is replaced with light that has a continuous spectrum. Simulating this process of averaging requires Mie calculations at many wavelengths.

As mentioned above, natural atmospheric effects involve scattering from millions of drops of varying sizes. Having calculated the data for many values of r to produce a Lee diagram for monodisperse drops, one can easily generate a Lee diagram for disperse drops. Figure 8 shows the results for drops with a log-normal size distribution with a standard deviation of 20%. Comparison of Fig. 7 with Fig. 8 shows that this variability in drop sizes suppresses the rainbow's supernumeraries, especially for $r >$ 100 μm.

Figures 9(a) and 9(b) show simulations of primary and secondary rainbows caused by scattering of sunlight from water drops of $r = 200$ μm and $r = 500$ μm, respectively (as might be observed with a 35-mm film camera with a lens of focal length 70 mm). In nature, Alexander's dark band would be much lighter than shown in Fig. 9, because these simulations ignore other sources of light such as diffuse or multiple scattering, skylight, and reflected light. Such mechanisms have been widely studied, but recent research by Gedzelman and Lock is particularly relevant because it combines Mie theory with multiple scattering.[19,23,24] Furthermore, Fig. 9 is based on the unrealistic assumption of monodisperse raindrops: Variations in drop size will inevitably reduce the visibility of the supernumerary arcs.

For scattering of sunlight from natural water drops, it seems that the ripples calculated so exactly by Mie theory must be smoothed away, thus giving results similar to Airy theory. Consequently, it is easy to understand why the Airy method is preferred for simulation of rainbows. Lee's paper concludes as follows:

> Thus, far from being an outdated irrelevancy, Airy theory shows itself to be a simple, quantitatively reliable model of the natural rainbow's colors and luminances. Provided that we restrict ourselves

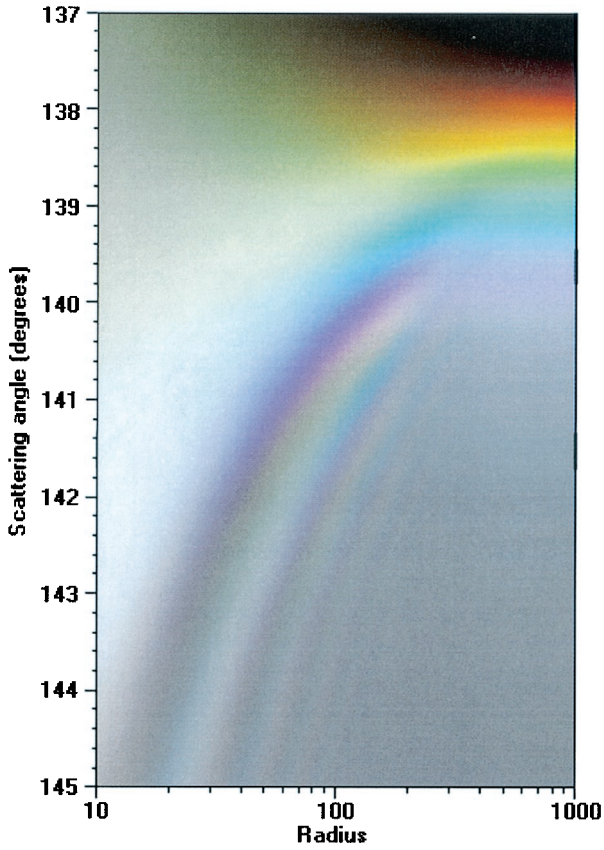

Fig. 8. As in Fig. 7, except that drops of nominal radius r have a log-normal size distribution with a standard deviation of 20% of the nominal value.

to spectrally integrated luminances (or radiances), it can be used to predict accurately the visual appearance of most naturally occurring water-drop bows and supernumeraries. Equally important, we see that Mie theory for monodispersions should not always be the model of first resort, as it produces details not seen in the natural rainbow and does so with much more computational effort than Airy theory. (Ref. 17. p. 1518)

3. Simulation of Coronas and Glories

Figure 10 shows MiePlot simulations of the corona and the glory for $r = 10$ μm. In real life it is difficult to observe the corona around the Sun, because the glare of the Sun obscures the colored rings. Hence the brightness of the simulated corona in Fig. 10 has been increased by a factor of 20 so that the Sun and its immediate surroundings are overexposed. The corona and the glory have different sizes, but the sequence of colors is almost identical. The key differences are that, for $r = 10$ μm, the glory has a dark ring around $\theta = 179.3°$ and that, in general, the outer rings of glories are relatively bright compared with those of coronas.

Although similar in appearance, these two phenomena are caused by completely different mechanisms. The corona is the result of simple diffraction and, thus, can be satisfactorily modeled by use of Bessel functions. On the other hand, there are no simple theories to explain the glory. Following the pioneering research in 1947 of van de Hulst,[25] the modern consensus is that the glory is caused by a combination of surface waves and rays that have undergone many internal reflections.[26–28]

Figure 11 shows simulations of the glory caused by scattering of unpolarized sunlight from a water drop of $r = 10$ μm with the specified number of wavelengths. At least 600 wavelengths are needed to achieve consistent results. Figure 11 indicates that the inner red ring of the glory occurs at approximately $\theta = 177.6°$, with a second red ring at 176.3° and much fainter red rings at 174.4° and 172.5°.

Figure 12 is a Lee diagram showing how the appearance of the glory varies with the radius r of the water drop. The sequence of ring colors is essentially independent of r. To a first approximation, the

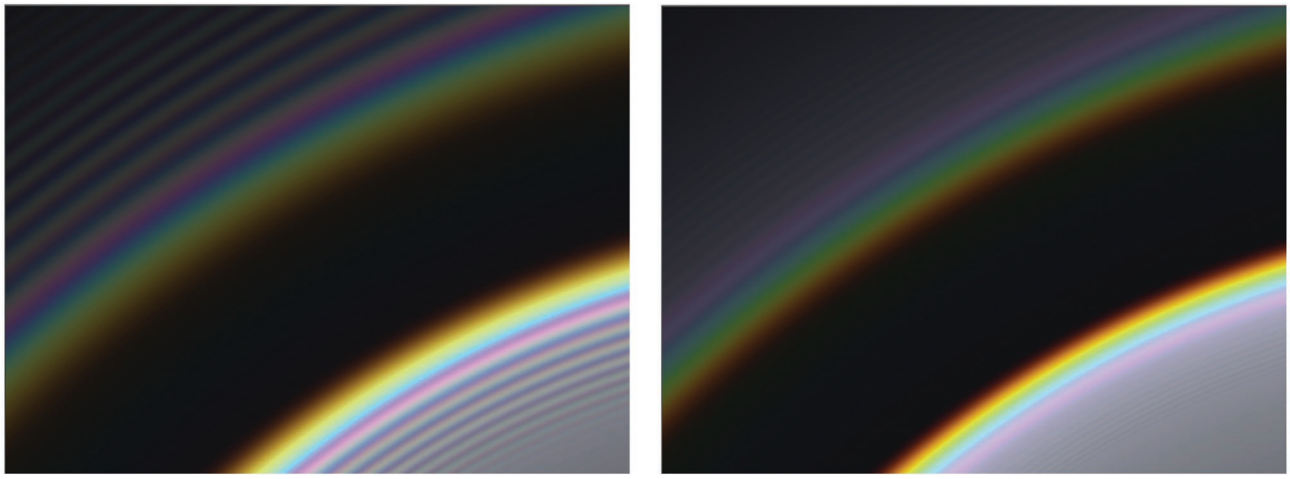

Fig. 9. (a) Simulation of primary and secondary rainbows caused by scattering of unpolarized sunlight from $r = 200$ μm water drops. (b) Simulation of primary and secondary rainbows caused by scattering of unpolarized sunlight from $r = 500$ μm water drops.

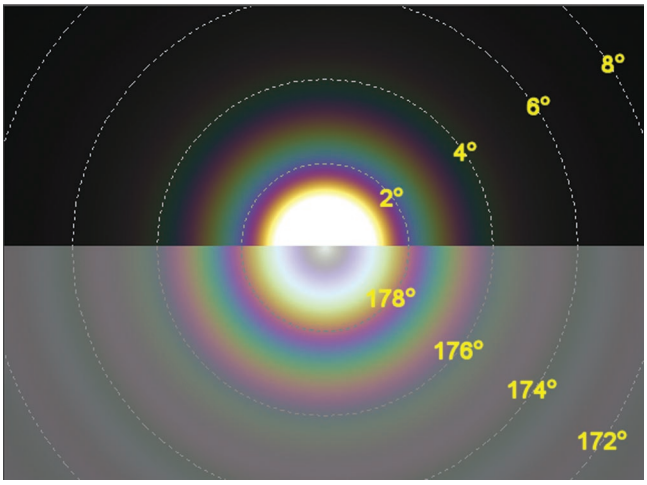

Fig. 10. Simulation of corona (top) and glory (bottom) caused by scattering of unpolarized sunlight from $r = 10$ μm water drops.

radius of a given ring from the antisolar point ($\theta = 180°$) is inversely proportional to r; for example, the four inner red rings have radii (measured in degrees) of approximately $24/r$, $37/r$, $56/r$, and $75/r$ (where r is measured in μm).

The MiePlot program allows comparisons of simulations with photographs of atmospheric optical effects. Figure 13 shows a digital image of a glory observed from a commercial aircraft, together with a superimposed MiePlot simulation of scattering of sunlight by water drops with $r = 4.8$ μm. Apart from adding a background color roughly matching that of the original image, no other adjustments have been made to the simulation. It should be noted that the close agreement between the original image and the simulation does not necessarily prove that the simulation is accurate, because we have no independent confirmation of the size of the water drops causing the glory. Nevertheless, another simulation for $r = 4.7$ μm produces rings that are larger than the observed rings, whereas a simulation for $r = 4.9$ μm produces rings that are smaller. Subject to the accuracy of the camera's calibration, we can be moderately confident that water drops of ~4.8 μm were responsible for this particular glory.

Figure 14 shows a digital image of a faint glory surrounded by a portion of a cloudbow, in which there is a dark ring around $\theta = 144°$ and an almost-white ring around $\theta = 141°$. Figure 15 is a MiePlot simulation of the same image based on scattering of sunlight by water drops with $r = 20$ μm, plus a uniform background color. The details provided by the simulation are much clearer than in the original image, but it is reasonable to assume that water drops with $r \approx 20$ μm were dominant in the observed clouds.

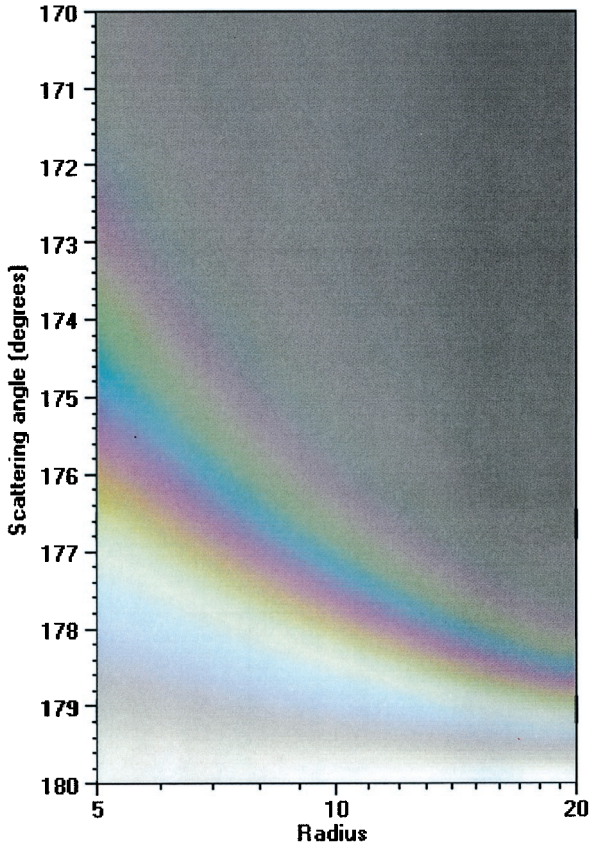

Fig. 12. Lee diagram of the glory caused by scattering of unpolarized sunlight from water drops of nominal radius r with a log-normal size distribution and a standard deviation of 5% of the nominal value.

4. Sources of Error

Although Mie theory is rigorous, various assumptions made within the MiePlot program can affect the validity of simulations of atmospheric optical effects. One assumption mentioned above concerns the spectral radiance of sunlight: Different models of spec-

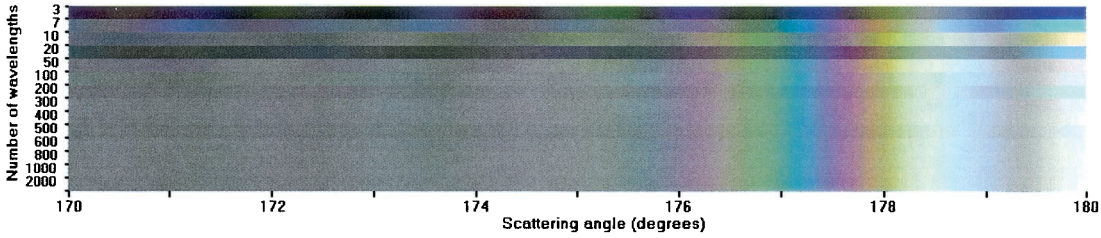

Fig. 11. Simulation of the glory caused by scattering of unpolarized sunlight from $r = 10$ μm water drops with the specified number of wavelengths equally spaced between 0.38 and 0.7 μm.

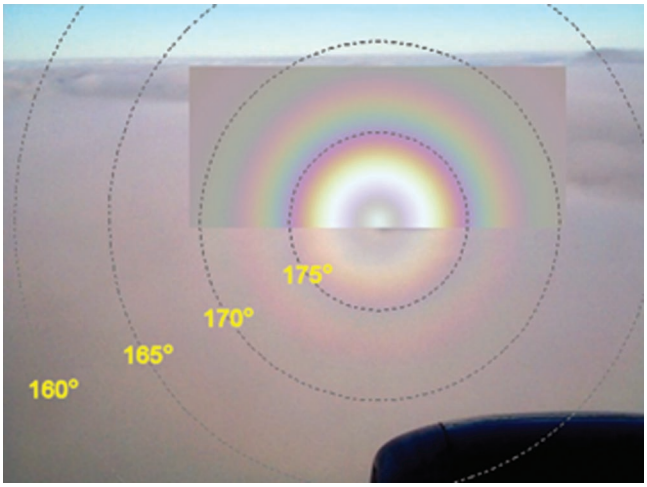

Fig. 13. Digital image of a glory with a superimposed simulation of scattering of unpolarized sunlight from $r = 4.8$ μm water drops.

tral radiance would obviously affect the color balance of simulations.

It is also necessary to define the refractive index n of water as a function of wavelength λ. There are surprisingly wide variations in the value of n quoted by various sources.[29–33] For example, the quoted values of n for $\lambda = 400$ nm vary between 1.3427 and 1.3498, corresponding to primary rainbow angles of 139.3° and 140.3°. Because most atmospheric effects are dependent on the absolute and relative values of n as a function of λ, such differences are, to say the least, disconcerting. The MiePlot program now allows the user to select one of several equations for n as a function of λ, but the default equation is that defined by the International Association for the Properties of Water and Steam.[33]

Even if the Mie simulations could be made mathematically precise, there is a substantial problem with colorimetry. First, it is necessary to define the colors corresponding to specific wavelengths of light in terms of RGB values used within the computer.[34] The MiePlot program uses the simple algorithm devised by Bruton.[35] Second, full-color simulations depend very much on the characteristics of the display devices, such as computer screens, projectors, or printers. In practice, differences in the inherent characteristics of computer displays (e.g., primary colors and gamma) are compounded by user settings, such as brightness, contrast, and color balance. Consequently, simulations in color can look dramatically different on different equipment. Further research is needed to address both these issues.

5. Conclusions

Mie theory provides a rigorous solution to the problem of scattering of sunlight from spherical raindrops, but it involves heavy computation. Simpler theories, such as Airy theory for rainbows or Bessel functions for coronas, can give almost identical results with much less computation. In some respects, using Mie theory can be equivalent to using a sledgehammer to crack a nut. Nevertheless, Mie theory remains the benchmark against which other theories are judged, and it is an invaluable tool for simulation of glories.

Advances in computer power mean that Mie theory can be used to produce full-color simulations of atmospheric optical effects. This paper has described the MiePlot computer program, which is freely available from the author. On a modern personal computer this program can produce simulations of glories and fogbows within a few minutes, whereas detailed simulations of rainbows might take 1 h or so.

Calculations with Mie theory can be erroneous if the scattering of a continuous spectrum is modeled by a small number of discrete wavelengths. For example, Mie calculations require ~600 wavelengths for simulation of the glory for $r = 10$ μm or 30 wavelengths for simulation of the primary rainbow for $r = 100$ μm.

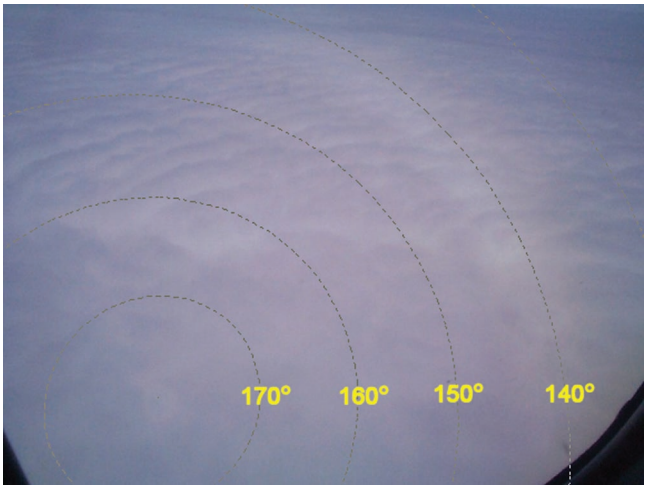

Fig. 14. Digital image of a faint glory and a cloudbow.

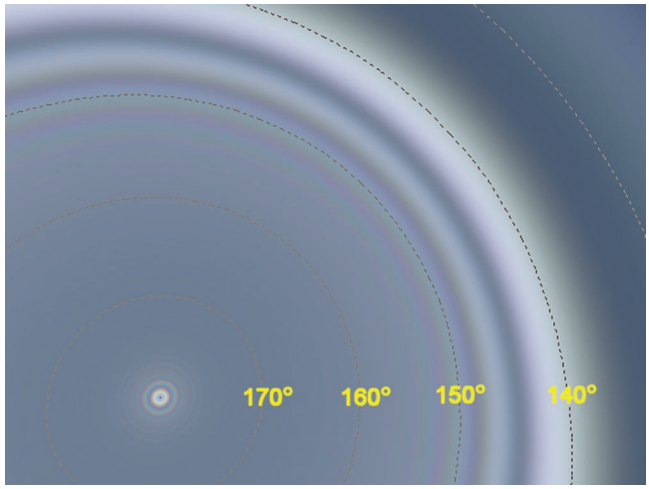

Fig. 15. Simulation of scattering of unpolarized sunlight from $r = 20$ μm water drops.

Other sources of errors include

- uncertainty about the values of refractive index n as a function of wavelength λ;
- colorimetry issues associated with display devices;
- relative intensity of the solar radiance as a function of λ;
- the effects of indirect illumination, such as multiple scattering, have been ignored.

Despite these potential sources of error, comparison of MiePlot simulations with digital images of natural glories is encouraging.

The author expresses his gratitude to Raymond Lee Jr. for his stimulating paper[17] and for his personal encouragement. Les Cowley provided invaluable suggestions and feedback during the writing and testing of the MiePlot program.

References

1. C. B. Boyer, *The Rainbow: From Myth to Mathematics* (Princeton University, Princeton, N.J., 1987; reprint of 1959 Thomas Yoseloff edition).
2. R. L. Lee, Jr., and A. B. Fraser, *The Rainbow Bridge: Rainbows in Art, Myth, and Science* (Penn State, University Park, Pa., 2001).
3. G. B. Airy, "On the intensity of light in the neighbourhood of a caustic," Trans. Cambridge Philos. Soc. **6,** Part 3, 397–403 (1838).
4. G. Mie, "Beitrage zur Optik trüber Medien, speziell kolloidaler Metallosungen," Ann. Phys. Leipzig **25,** 377–445 (1908).
5. H. C. van de Hulst, *Light Scattering by Small Particles* (Dover, New York, 1981; reprint of 1957 Wiley edition), pp. 167–171.
6. Ref. 5, pp. 152–153.
7. H. M. Nussenzveig, "The theory of the rainbow," in *Atmospheric Phenomena* (Freeman, San Francisco, Calif., 1980), pp. 60–71.
8. H. M. Nussenzveig, "Complex angular momentum theory of the rainbow and the glory," J. Opt. Soc. Am. **69,** 1068–1079 (1979).
9. C. F. Bohren and T. J. Nevitt, "Absorption by a sphere: a simple approximation," Appl. Opt. **22,** 774–775 (1983).
10. J. V. Dave, "Scattering of visible light by large water spheres," Appl. Opt. **8,** 155–164 (1969).
11. C. F. Bohren and D. R. Huffman, *Absorption and Scattering of Light by Small Particles* (Wiley, New York, 1983).
12. K. Liou and J. E. Hansen, "Intensity and polarization for single scattering by polydisperse spheres: a comparison of ray optics and Mie theory," J. Atmos. Sci. **28,** 995–1004 (1971).
13. S. T. Shipley and J. A. Weinman, "A numerical study of scattering by large dielectric spheres," J. Opt. Soc. Am. **68,** 130–134 (1978).
14. A. Ungut, G. Grehan, and G. Gouesbet, "Comparisons between geometrical optics and Lorenz–Mie theory," Appl. Opt. **20,** 2911–2918 (1981).
15. R. T. Wang and H. C. van de Hulst, "Rainbows: Mie computation and the Airy approximation," Appl. Opt. **30,** 106–117 (1991).
16. E. A. Hovenac and J. A. Lock, "Assessing the contributions of surface waves and complex rays to far-field Mie scattering by use of the Debye series," J. Opt. Soc. Am. A **9,** 781–795 (1992).
17. R. L. Lee Jr., "Mie theory, Airy theory, and the natural rainbow," Appl. Opt. **37,** 1506–1519 (1998).
18. R. K. Brandt and R. G. Greenler, "Color simulation of size-dependent features of rainbows," presented at the Seventh Topical Meeting on Meteorological Optics, Boulder, Colorado, 5–8 June 2001; available at http://www.asp.ucar.edu/MetOptics/Preprints.pdf.
19. S. D. Gedzelman and J. A. Lock, "Simulating coronas in color," presented at the Seventh Topical Meeting on Meteorological Optics, Boulder, Colorado, 5–8 June 2001; available at http://www.asp.ucar.edu/MetOptics/Preprints.pdf.
20. H. C. van de Hulst and R. T. Wang, "Glare points," Appl. Opt. **30,** 4755–4763 (1991).
21. X. Han, "Study of refractometry of rainbow and applications to the measurement of instability and temperature gradient of a liquid jet," Ph.D. dissertation (University of Rouen, Rouen, France, 2000), available at http://www.coria.fr/LESP/OP15/Han/TheseHan.htm.
22. G. P. Können and J. H. de Boer, "Polarized rainbow," Appl. Opt. **18,** 1961–1965 (1979).
23. S. D. Gedzelman and J. A. Lock, "Simulating coronas in color," Appl. Opt. **42,** 497–504 (2003).
24. S. D. Gedzelman, "Simulating glories and cloudbows in color," Appl. Opt. **42,** 429–435 (2003).
25. H. C. van de Hulst, "A theory of the anti-coronae," J. Opt. Soc. Am. **37,** 16–22 (1947).
26. T. S. Fahlen and H. C. Bryant, "Direct observation of surface waves on droplets," J. Opt. Soc. Am. **56,** 1635–1636 (1966).
27. Ref. 8, pp. 1073–1078.
28. W. T. Grandy, *Scattering of Waves from Large Spheres* (Cambridge University, Cambridge, UK, 2001).
29. D. K. Lynch and W. Livingston, *Color and Light in Nature* (Cambridge University, Cambridge, UK, 2001).
30. D. Segelstein, "The complex refractive index of water," M.S. thesis (University of Missouri, Kansas City, Mo., 1981).
31. G. W. C. Kaye and T. H. Laby, *Tables of Physical and Chemical Constants, and Some Mathematical Functions* (Longman, London, 1986).
32. P. Schiebener, J. Straub, J. M. H. L. Sengers, and J. S. Gallagher, "Refractive index of water and steam as function of wavelength, temperature and density," J. Phys. Chem. Ref. Data **19,** 677–717 (1990).
33. International Association for the Properties of Water and Steam, "Release on the refractive index of ordinary water substance as a function of wavelength, temperature and pressure" (1997), http://www.iapws.org/relguide/rindex.pdf.
34. G. Wyszecki and W. S. Styles, *Color Science: Concepts and Methods, Quantitative Data and Formulae*, 2nd ed. (Wiley, New York, 1982), pp. 138–139.
35. D. Bruton, "Color science" (1996), http://www.physics.sfasu.edu/astro/color/spectra.html.